*Polish Journal of Chemical Technology, 19, **4**, 128—136, 10.1515/pjct-2017-0079*

Green synthesis, characterization and antibacterial activities of silver nanoparticles from strawberry fruit extract

Saviour A. Umoren[1*], Alexis M. Nzila[2], Saravanan Sankaran[2], Moses M. Solomon[3], Peace S. Umoren[4]

[1]*King Fahd University of Petroleum and Minerals, Centre of Research Excellence in Corrosion, Research Institute, Dhahran 31261, Saudi Arabia*
[2]*King Fahd University of Petroleum and Minerals, Department of Life Sciences, College of Science, Dhahran 31261, Saudi Arabia*
[3]*University of Uyo, Department of Chemistry, Faculty of Science, Uyo, P.M.B. 1017 Uyo, Nigeria*
[4]*University of Uyo, Department of Medical Microbiology and Parasitology, Faculty of Clinical Sciences, Uyo, P.M.B. 1017 Uyo, Nigeria*
[*]*Corresponding author: e-mail: umoren@kfupm.edu.sa*

Silver nanoparticles (AgNPs) have been synthesized in the presence of Strawberry fruit extract (SBFE) at room temperature. The synthesized AgNPs was characterized by UV-vis spectroscopy, SEM, EDS, XRD, TEM and FTIR. The UV-vis spectra of the AgNPs show SPR band at 450 nm. TEM results indicate that AgNPs are spherical in shape and size range between 7–65 nm. Antibacterial activity of the synthesized AgNPs has been assessed against *Pseudomonas aeruginosa* and *Bacillus licheniformis*. The results show that AgNPs exhibit inhibitory effect and effect is a function of AgNPs concentration. The antibacterial activity of the prepared AgNPs has been compared with two antibiotics, amoxicillin and ciprofloxacin. It is found that the antibiotics perform better than AgNPs.

Keywords: strawberry fruit, silver nanoparticles, biosynthesis, characterization, antibacterial activity.

INTRODUCTION

Metal nanoparticles particularly silver nanoparticles (AgNPs) have attracted considerable attention in recent times because of their attractive properties related with the quantum size effect and their limitless applications in areas such as optics, catalysis, optoelectronics, chemical/biochemical sensing, biomedical, and nanostructure fabrication[1–5]. They can be synthesized by physical[6, 7, 8], chemical[9, 10, 11], or radiation-chemical[12, 13, 14, 15], methods. Although successes have been achieved with these techniques, environmental issues associated with most chemical substances used as reducing agents, technical laboriousness, and high financial demand have made these methods less attractive. Economical and eco-friendly synthetic route considered by researchers at present is biosynthesis using bacteria[16] fungi[17, 18] biomolecules[19] and extensively, plant parts[4, 20, 21, 22]. The use of plant extract in the synthesis of metal nanoparticles is of remarkable interest because they can act as reducing agents as well as capping agents in addition to their environmental friendliness, sustainability and cost-effectiveness.

It has been established[23–25] that silver ions, silver compounds and silver nanoparticles have antimicrobial and antiviral effects. As such, researchers have screened most plant mediated silver nanoparticles for their antimicrobial and antiviral effects. Padalia et al.[21] synthesized sliver nanoparticles using flower broth of *Tagetes erecta* as reductant by a simple and eco-friendly route and evaluated the synergistic antimicrobial potential of the AgNPs with various commercial antibiotics against Gram positive (*S. aureus* and *B. cereus*), Gram negative (*E. coli* and *P. aeruginosa*) bacteria and fungi (*C. glabrata, C. albicans, C. neoformans*). It was found that antifungal activity of AgNPs with antibiotics was better than antibiotics alone against the tested fungal strains and Gram negative bacteria. Gopinath et al.[4] prepared silver nanoparticles using *Tribulus terrestris* L. fruit bodies and observed antibacterial activity by Kurby-Bauer method with clinically isolated multi-drug resistant bacteria such as *Streptococcus pyrogens*, *Pseudomonas aeruginosa, Escherichia coli, Bacillus subtilis*, and *Staphylococcus aureus*. The synthesized nanoparticles were found to be spherical in shape, ranged between 16–28 nm in size, and showed high potency to the tested bacteria. Bindhu and Umadevi[5] reported high antimicrobial activity of *Hisbiscus cannabinus* leaf mediated nanoparticles against *Escherichia coli*, *Proteus mirabilis*, and *Shigella flexneri*. Sankar et al.[13] noted that silver nanoparticles achieved using aqueous extract of *Origanum vulgare* (Oregano) showed dose dependent response against human lung cancer A549 cell line (LD_{50-100} μg/mL). Also, Ahmed et al.[26] found recently that silver nanoparticles synthesized using aqueous leaves extract of *Skimmia laureola* at room temperature are potent against human pathogenic Gram-positive and Gram-negative bacteria.

Strawberry is of the genus *Fragaria* and cultivated mostly for its fruit. It is consumed either fresh or in such prepared foods as fruit juice, pies, ice creams, milkshakes, and chocolates[27]. Earlier reports have shown that strawberry consumption has the capacity to decrease cardiovascular disease risk and its phytochemicals possess anti-inflammatory or anticancer properties[27–29]. Our motivation towards synthesizing Strawberry mediated silver nanoparticles and testing for its antibacterial activity stemmed from these findings. Herein, we report the green synthesis of silver nanoparticles using extract of strawberry fruit and the potency of the nanoparticles against *Pseudomonas aeruginosa* and *Bacillus licheniformis*. The prepared nanoparticles were characterized by UV–vis, XRD, FTIR, TEM and EDS.

MATERIAL AND METHODS

Preparation of strawberry fruit extracts (SBFE)

25 g of freshly purchased Strawberry fruits were rinsed severally with distilled water and were then cut into small pieces followed by crushing with a mixer grinder by adding about 100 mL of distilled water into it. It was then filtered using Whatman no. 1 filter paper and the filtrate was centrifuged at 8.000 rpm for 10 min to remove fibrous impurities. Thereafter, the aqueous extract was refrigerated prior to use.

Synthesis of silver nanoparticles

Aqueous solutions (0.001 M and 0.01 M) of silver nitrate ($AgNO_3$) were prepared and used for the synthesis of the silver nanoparticles. Different concentrations (0.1–2.0 mL) of aqueous extract of Strawberry fruit were introduced into a 250 mL Ertenmeyer flask and appropriate amount of $AgNO_3$ (0.001 M or 0.01 M) was added. The reaction mixture was allowed to stand at room temperature for 24 h and to extended period up to 18 days to evaluate the effect of time on the nanoparticles formation. Silver nanoparticles were gradually formed during the period as was evident in the colour change of the reaction mixture (Fig. 1).

Characterization of silver nanoparticles

Uv–visible measurements

The spectral analysis for the development of AgNPs was observed using JASCO770-UV-vis spectrophotometer from 250 to 800 nm using a dual beam operated at a resolution of 1 nm with a scan rate of 200 nm/min at ordinary temperature. Sharp peak in the range of visible region of the electromagnetic spectrum indicates the formation of AgNPs.

SEM analysis

Scanning electron microscopy (SEM) analysis was performed using the JEOL JSM-6610 LV instrument. Thin films of the sample were prepared on a carbon coated gold and platinum grid by simply dropping a small amount of the sample on the grid.

EDS analysis

Samples were prepared by depositing a drop of colloidal solution on an aluminum grid sample holder and drying at normal temperature. The elemental composition of the sample was analyzed with energy dispersive spectroscopy (EDS) coupled to the SEM JEOL JSM-6610 LV

XRD analysis

AgNPs solution was centrifuged at 10.000 rpm for 30 min. The solid residues of AgNPs were washed twice with distilled water and then re-dissolved in absolute ethanol and evaporated to dryness at 353 K to get powder AgNPs which was used for X-ray diffraction (XRD) measurements. The XRD patterns were recorded on Rigaku Mini-flex II system using nickel filtered Cu Kα radiation $\lambda = 1.5406^{o}A$ at 40 kV and 30 mA.

TEM analysis

The morphological examination of the shape and size of silver nanoparticles was carried out using transmission electron microscopy (TEM). The drop of silver nanoparticle solution was loaded on carbon-coated copper grid and allowed to dry for an hour. The TEM micrograph images were recorded on JEOL instrument JEM-2100F instrument on carbon coated copper grids with an accelerating voltage of 200 kV.

FTIR analysis

Fourier transformed infrared (FTIR) spectra of AgNPs samples were recorded with the aid of Fourier transformed infrared (Perkin Elmer 16F PC FTIR) spectrometer. The FTIR spectrum ranged from 4000 to 450 cm^{-1} at a resolution of 4 cm^{-1} by making a KBr pellet with the solid residue of AgNPs obtained by evaporating to dryness the colloidal solution of the synthesized nanoparticles in a petridish at 50°C.

Zeta potential measurement

The zeta potential of the synthesized AgNPs was determined in water as dispersant using Zetatrac (Microtrac, USA).

Bacterial culture

Two bacterium strains were employed in this study, and these are the gram-*Pseudomonas aeruginosa* N7B1 and the gram+ *Bacillus licheniformis* (Gene Bank accession numbers GI 482716237 and 540360856 respectively). These strains were isolated from petroleum contaminated shore lines of the Arabian Gulf of Saudi Arabia. They were cultivated in Luria broth (LB) medium (containing 10 g L of 1 peptone, 5 g L of 1 yeast extract, and 10 g L of 1 sodium chloride) in a shaker-incubator at 37°C, 120 rpm for 2–3 days, and the growth was monitored by measuring the absorbance (optical density [OD]) of culture at the wavelength of 600 nm, the standard wavelength to measure bacterial growth. The OD measurements were carried out using the APEL PD-303 UV spectrophotometer (Japan). The growth was also measured by visual observation of the turbidity of the culture. To quantify individual colonies, bacteria were streaked on a solid medium of Luria broth medium supplemented with1 % agar, incubated at 37°C for 24 h, and colonies were counted and the results represented as colony forming unit (CFU/ml of the culture).

Antibacterial assay

Two approaches were employed to assess the antibacterial activity of the nanoparticles. The first was the "cup and plating" method, adapted from Rios et al.[30], a gross estimation of antimicrobial activity. The experiment was carried out in solid medium, and after spreading 100 μL of a bacteria culture (containing 10^6 CFU/mL) on the agar plate, the plate was cupped at the center, with a formation a small hole (around 5mm diameter and 2 mm height) in which the antimicrobial agent was added from. The antimicrobial activity was measured by the diameter of the inhibition zone (disc diffusion). The higher the diameter of the inhibition zone, the higher the activity of the antimicrobial agent.

The second approach was based on the use of liquid medium to establish the antibacterial activity of the nanoparticles. A serial dilution (by factor of 10 for a total of 4 dilutions) of nanoparticles (starting from 0.01 M) was prepared using a fresh culture medium, and 200 μL of each were added in a 5mL LB culture tubes. The tubes were incubated at 37°C in a shaker at 250 rpm for 24 h. Positive control tubes consisted of bacteria culture without antibacterial agents, while negative control contained the antimicrobial agent but without bacteria. In addition, two antibiotics, amoxicillin and ciprofloxacin were used as references. The growth of bacteria after 24 h was associated with an increase in turbidity, and this turbidity was assessed visually. The minimum inhibitory concentration (MIC), which also reflects the bacteriostatic effect, was the lower concentration at which no turbidity was visualized, in comparison with the positive and negative controls. The turbidity reflected the presence of both viable and dead bacteria. To assess the presence of viable bacteria, 100 μL of each culture was spread on the agar LB plate and incubated at 37°C for 24 h. Viable bacteria were counted, and data represented as colony forming unit (CFU). The minimum concentration of antibacterial agent that prevented bacteria growth in the solid plate medium was referred to as minimum bactericidal concentration (MBC). These methods used for assessing MIC and MBC were described elsewhere[31].

RESULTS AND DISCUSSION

UV-vis analysis

By mixing Strawberry fruit extract (SBFE) with $AgNO_3$ solution and allowing it to stand at ordinary temperature for 24 h, the initial yellow coloration turned dark brown and deepened after 96h of reaction time (Fig. 1). This change could possibly be due to excitation of Surface Plasmon Resonance (SPR) during the formation of silver nanoparticles[1, 32]. To ascertain whether or not the color change was due to reduction of Ag^+ to Ag^0 during the formation of AgNPs, UV-vis analysis of the mixture was conducted. UV-vis spectroscopy has enjoyed high patronage in the analysis of silver nanoparticles because of the uniqueness of AgNPs peak at about 380–450 nm arising from SPR transition[33, 34]. Figure 2 shows the UV–vis spectra recorded as a function of concentration of SBFE extract in a reaction with an aqueous solution of

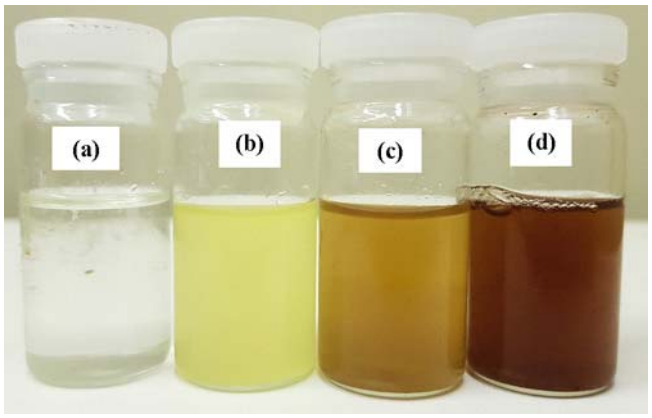

Figure 1. Photograph of (a) $AgNO_3$ solution, (b) $AgNO_3$ + SBFE extract, (c) AgNPs after 24 h and (d) AgNPs after 96 h

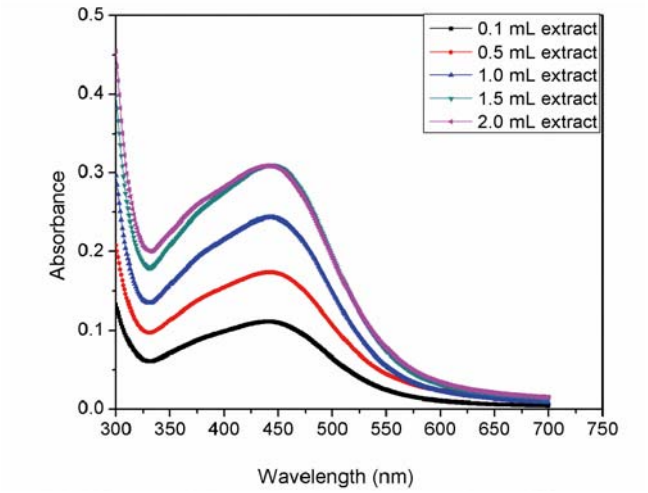

Figure 2. UV–vis spectra recorded as a function of concentration of SBFE extract in a reaction with an aqueous solution of 1mM $AgNO_3$ after 24 h

1mM $AgNO_3$ after 24 h. From the figure, the absorption bands typical of SPR transition can be clearly seen at about 450 nm. However, the intensity of the absorption band is a function of SBFE concentration and may mean increasing number of nanoparticles. According to Ghaffari-Maghaddam and Hadi-Dabanlou[20], the SPR band is influenced by the size, shape, morphology, composition, and the dielectric environment of the synthesized AgNPs.

To study the influence of silver ion concentration and reaction time, UV-vis experiments were performed using different concentrations of $AgNO_3$ at different reaction times. The UV-vis spectra obtained for AgNPs synthesized using aqueous SBFE at 1 day and 18 days reaction with 0.01 and 0.001 M aqueous $AgNO_3$ solutions respectively are shown in Figure 3. It is obvious from the figure that at short reaction time (1 day), the absorption peaks for both AgNPs synthesized from 0.01 and 0.001 M $AgNO_3$ respectively are not very prominent. This could be interpreted to mean fewer AgNPs at this reaction time. As the reaction time prolonged to 18 days, the absorption peaks become sharp and very prominent but with the intensity of the AgNPs synthesized from 0.01 M $AgNO_3$ being higher than that prepared from the lower concentration of $AgNO_3$. This means that at this reac-

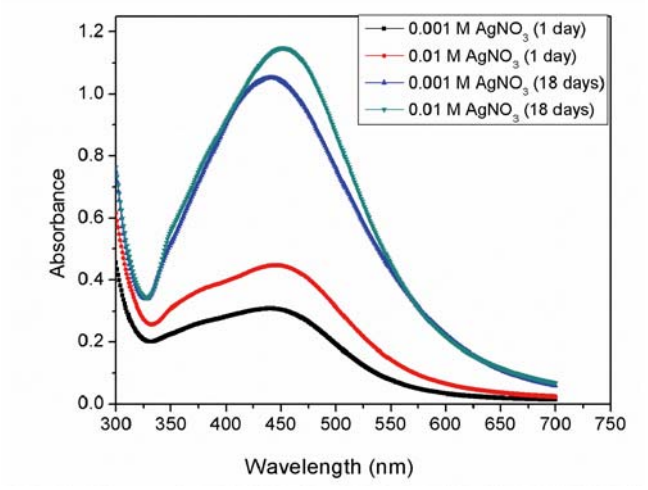

Figure 3. UV-visible spectra of AgNPs synthesized using aqueous SBFE at 1 day and 18 days reaction time with 0.01 and 0.001 M aqueous $AgNO_3$ solution

tion time, much AgNPs which were stable and without much aggregation were formed. This is also evident in the high negative value of zeta potential (–54.46 mV) (Table 1). As explained by Prathna et al.[35] such stability arises from potential barrier that develops as a result of competition between weak van der Waal forces of attraction and electrostatic repulsion.

Table 1. Zeta potential result for AgNPs formed from strawberry fruit extract

Parameter	Values
Mobility	–4.25 u/s/V/cm
Zeta potential	–54.46 mV
Charge	–0.09548 fC
Polarity	Negative
Conductivity	1.214 µS/cm

The mechanism of biosynthesis of metal nanoparticles using plant extracts is a complex one because of the complexity involved with the composition of plant extract. Plant extract is a rich source of complex bioactive molecules such as enzymes, proteins, polysaccharides, flavonoids, amino acids, vitamins, etc.[36] which can act as reducing and stabilizing agents. Although a general mechanism for plant mediated metal nanoparticles is difficult because of the above stated reason, scientists have attempted to pinpoint at the major phytochemicals in plant which could be responsible for the conversion of metal ion to elemental metal during metal nanoparticles synthesis. Chowdhury et al.[1] proposed that the synthesis of water-dispersible AgNPs at room temperature using green *carambola* (Star fruit) extract was initiated by the polysaccharides having the general formula $C_x(H_2O)_y$, which acted as the reducing agent according to the reaction:

$$2Ag^+ + C_x(H_2O)_y + H_2O \rightarrow 2Ag^0 + (C_xH_{2y-1}O_{y+1})^- + 3H^+ \quad (1)$$

Bindhu and Umadevi[5] reported that ascorbic acids present in *Hisbiscus cannabinus* leaf extract were responsible for the reduction of silver ions to elemental silver during the synthesis of AgNPs using the leaf extract. Ghaffari-Moghaddam and Hadi-Dabanlou[20] submitted that the green synthesis of AgNPs using *Crataegus douglasii* fruit extract was possible due to the oxidation of aldehydes present in the fruit extract to carboxylic acids. The investigation of Cordenunsi et al.[37] into the chemical composition of Strawberry fruit revealed that the fruit contains ascorbic acid, soluble sugars (fructose, sucrose, and glucose), phenolics, and flavonoids in appreciable amount. These phytochemicals could be responsible for the conversion of Ag^+ to Ag^0 in the present study.

SEM/EDS analyses

Figure 4 shows scanning electron microscopy (SEM) images of synthesized AgNPs with (a) 0.001 M and (b) 0.01 M $AgNO_3$ solution and their corresponding energy dispersive X-ray spectroscopy (EDS) images after 24 h reaction time. As could be clearly seen in Figure 4, Strawberry fruit extract successfully reduced $AgNO_3$ to AgNPs and the nanoparticles are spherical in shape from 0.001 M $AgNO_3$ concentration and of mixed shape from the 0.01 M $AgNO_3$ concentration. Also the sizes of the AgNPs are larger from the higher concentration of $AgNO_3$ (0.01 M) than the lower concentration (0.001 M) studied. In the corresponding EDS images (Fig. 4a, b), typical optical absorption peak of metallic

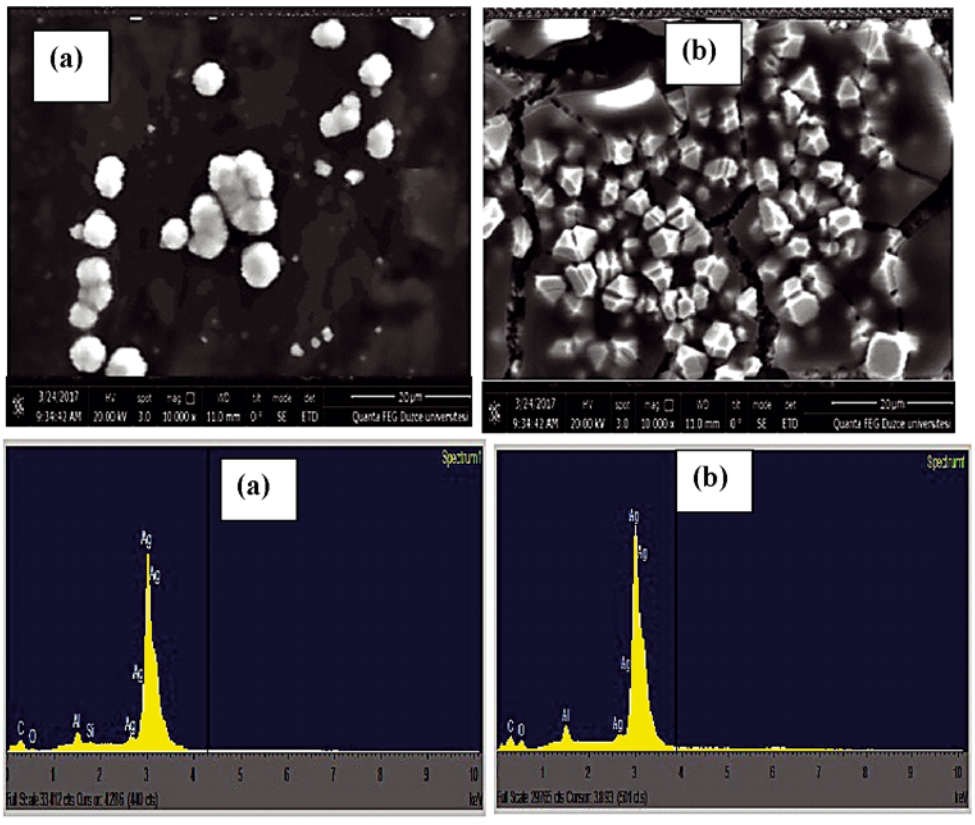

Figure 4. SEM images of synthesized AgNPs with (a) 0.001 M and (b) 0.01 $AgNO_3$ and their corresponding EDX images after 24 h reaction time

silver nanocrystals at 3 keV[1, 38] can be visibly seen, thus confirming the formation of AgNPs. The Al peak also seen in Figure 4(b) arose due to the Al grid while the C and O peaks come from organic phytoconstituents in the fruit extract.

XRD analysis

The XRD pattern of Ag nanoparticles synthesized by treating 5 mL aqueous SBFE with 0.001 M aqueous $AgNO_3$ solution is presented in Figure 5. The four peaks are observed at $2\theta = 38.5^o$, 45.7^o, 65.6^o, and 78.7^o and can be indexed to the (111), (200), (220), and (311) of a pure silver (JCPDS Card No. 04-0783), thus supporting the strawberry fruit extract biosynthesis of AgNPs proposed from other characterization methods. However, two peaks are observed at $2\theta = 28^o$ and 32^o respectively. These might infer the presence of impurities in the biosynthesized AgNPs. As posited by Lateef et al.[39], mineral elements in plant extract may converge as impurities on the surface of a biosynthesized AgNPs.

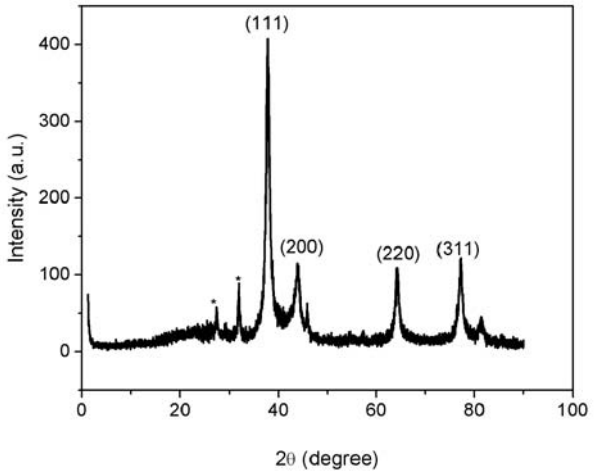

Figure 5. XRD patterns of Ag nanoparticles synthesized by treating 5 mL aqueous SBFE with 0.001 M aqueous $AgNO_3$ solution

TEM analysis

The morphology of the synthesized SBFE mediated AgNPs was also observed with the aid of transmission electron microscope (TEM). Figure 6 shows the TEM micrographs for AgNPs prepared by treating 5 mL of SBFE with 0.01 M $AgNO_3$ solution at (a) 100 nm, (b) 50 nm, and (c) selected area electron diffraction (SAED) patterns. Similar TEM pictures for AgNPs synthesized by treating 5 mL of SBFE with 0.001 M $AgNO_3$ solution are given in Figure 7. It is observed from the figures that the AgNPs formed are well dispersed and are spherical in shape, thus corroborating the SEM results (Fig. 4a). The crystalline nature of the nanoparticles established from the XRD results (Fig. 5) is further proven by the bright circular spots seen in the SAED patterns in Figures 6c and 7c which correspond to (111), (200), (220), and (311) Bragg reflection planes[5]. A comparison of the TEM micrographs in Figure 6a ,b to Figure 7a, b reveals bigger AgNPs in Figure 6a, b than in Figure 7a, b which is in conformity with the UV-vis results in Figure 3.

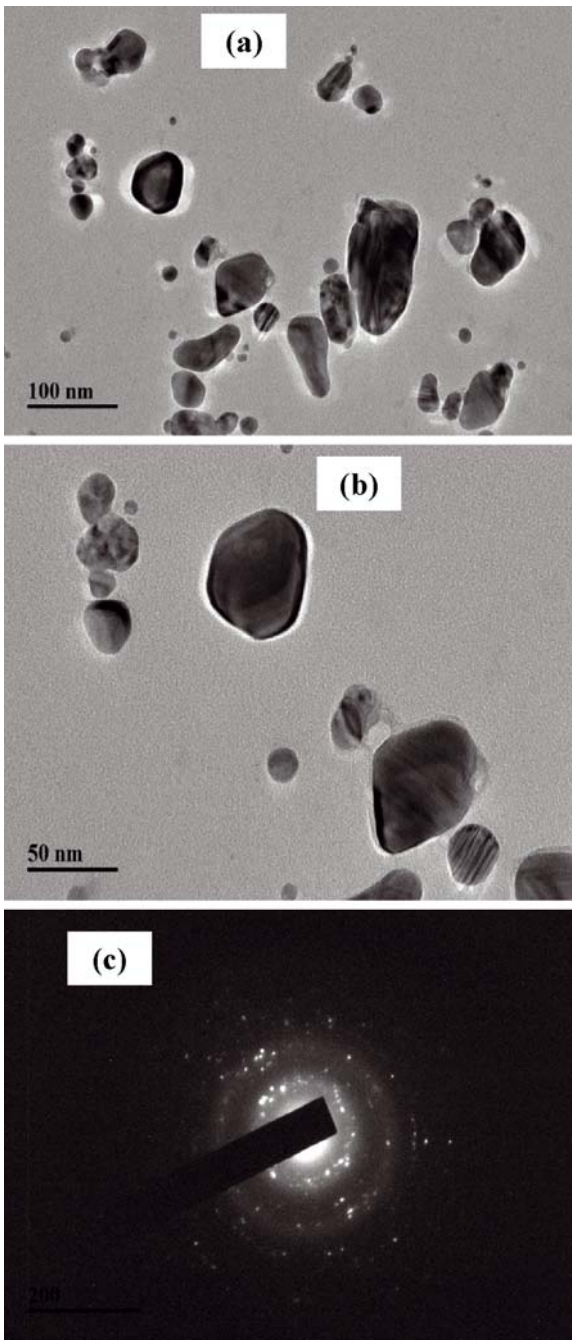

Figure 6. TEM micrographs for AgNPs using 0.001 M $AgNO_3$ solution at (a) 100 nm, (b) 50 nm magnifications and (c) SAED patterns of AgNPs

FTIR analysis

To identify the possible bioactive molecules in strawberry fruit extract responsible for the reduction of Ag^+ to Ag^0 and the stabilization mode of the AgNPs, FTIR measurements were carried out. Figure 8 shows the FTIR of AgNPs synthesized by treating 5 mL aqueous SBFE with (a) 0.001M, (b) 0.01 M aqueous $AgNO_3$ solution and (c) SBFE alone. For the spectra in Figure 8a and b, notable peaks are at 3400, 1720, 1382, and 1070 cm^{-1}. The absorption peak at 3400 cm^{-1} signifies OH stretching mode of polyols present in the fruit extract and are in some degree of hydrogen bonding. This hydrogen bonding may be responsible for the stabilization of the silver nanoparticles. Authors have given similar submission[1, 40]. The peak at 1720 cm^{-1} arose from C=O stretching of ketones in ascorbic acid present in the fruit extract. Cordenunsi et al.[37] had quantitatively

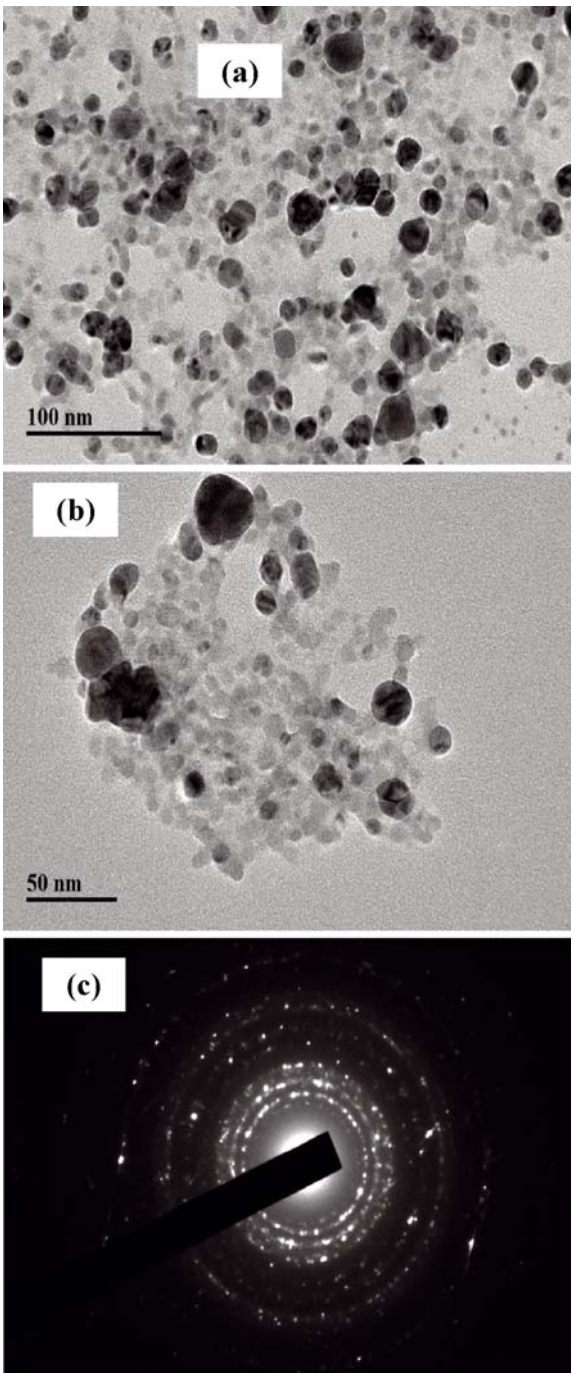

Figure 7. TEM micrographs for AgNPs using 0.01 M $AgNO_3$ solution at (a) 100 nm, (b) 50 nm magnifications and (c) SAED patterns of AgNPs

shown that strawberry fruit contained ascorbic acid in an appreciable quantity. The C-O stretching and OH out-of-phase plane deformation signals of ascorbic acid appear at 1382 and 1070 cm^{-1} respectively. Compared with the SBFE spectra in Figure 8c, the striking difference is on the intensity of the C-O stretching band at 1382 cm^{-1} and the position of the C=O stretching peak. It can be seen that the C-O peak is more intense in the SBFE spectra (Fig. 8c) than in the AgNPs spectra (Fig. 8a and b). Also, the C=O stretching peak appeared at 1610 cm^{-1} in the SBFE spectra but was shifted to 1720 cm^{-1} in the silver nanoparticles spectra. This obvious changes in the intensity of C-O peak and position of C=O peak indicate that ascorbic acid present in SBFE played a significant role in the conversion process of silver ions to elemental silver. Also, by comparing Figure 8a and (b), the influence of silver ions concentration can be seen. All the absorption peaks in the FTIR spectra in Figure 8b are stronger than those in Figure 8a which is in perfect agreement with the results from the other characterization methods and further support the submission that 0.01 M $AgNO_3$ gives rise to bigger AgNPs than 0.001 M $AgNO_3$.

Zeta potential measurement

Zeta potential is defined as the potential difference between the dispersion medium and the stationary layer of fluid attached to the dispersed particle. It is a key indicator of the stability of colloidal dispersions. The magnitude of the zeta potential indicates the degree of electrostatic repulsion between adjacent, similarly charged particles in dispersion. The zeta potential of the synthesized AgNPs was determined in water as dispersant. The result obtained from the zeta potential measurement is displayed in Table 1. From the table, the zeta potential is seen to be negative with numerical value of 54.46 mV. The high value indicates existence of repulsion among charged particles resulting in increased stability of the formulation[41]. The negative potential value could be possibly attributed to the capping of the bio-organic components present in the extract[42].

Antibacterial activity

The gross activity of the AgNPs was established grossly by employing the cup-plate experiment and the studies were carried out in duplicate. Two concentrations of

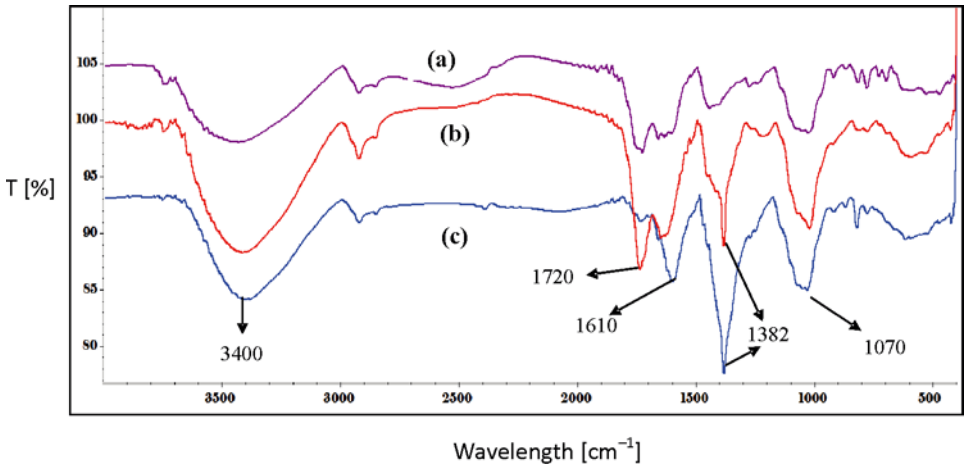

Figure 8. FTIR of AgNPs synthesized by treating 5 mL aqueous SBFE with (a) 0.001M, (b) 0.01 M aqueous $AgNO_3$ solution and (c) SBFE alone

the nanoparticles were tested, 4×10^{-4} and 4×10^{-5} M. As shown in Table 2, against *Pseudomonas aeruginosa*, AgNPs inhibited the bacteria growth on a diameter of 3 mm at 4×10^{-4} M, and this value decreased to 2.5 at a lower concentration (4×10^{-5} M). Likewise, *Bacillus licheniformis* growth was inhibited on a diameter of 4.5 and 3.5 mm with AgNPs synthesized using 4×10^{-4} and 4×10^{-5} M solution respectively. These preliminary data indicate that AgNPs has antibacterial activity.

Table 2. Assessment of antimicrobial effect of AgNPs, using the cup plate experiments. Values represent the diameter (in mm) of the inhibition zone. The tested concentrations are 4 ×10–4 and 4 ×10–5 for nanoparticles

Microorganisms	AgNPs	
	4×10^{-4} M	4×10^{-5} M
Pseudomonas aeruginosa	3.0	2.5
Bacillus licheniformis	4.5	3.5

To quantify this anti-bacterial activity, bacteria inhibition growth was carried out in liquid medium. The data show that low concentrations of AgNPs down to 4×10^{-5} M (for *P. aeruginosa*) and 4×10^{-7} M (for *B. licheniformis*) inhibited growth, based on visual turbidity (Table 3a). Thus, MIC for *P. aeruginosa* and *B. licheniformis* were 4×10^{-5} and 4×10^{-7} M respectively (Table 4). On the other hand, MIC for the 2 reference antibiotics were lower, with amoxicillin values of 5×10^{-7} and 5×10^{-8} M against *P. aeruginosa* and *B. licheniformis* respectively; while values pertaining to ciproflaxicin were 10^{-8} M for the 2 strains (Table 3b, c and Table 4). Further investigations on the ability of these bacteria to inhibit growth in solid agar medium showed the minimum concentrations of AgNPs at which growth is inhibited, which is equivalent to MBC, was 4×10^{-5} M (Table 3 a and Table 4). In line with MIC results, lower MBC values were obtained for the 2 antibiotics. Indeed, amoxicillin MBC were 10^{-8} M for both strains, while values of cirprofloxacin of 10^{-7} and 10^{-9} M corresponded to *P. aeruginosa* and *B. licheniformis* respectively (Table 3 b, 3 c, Table 4).

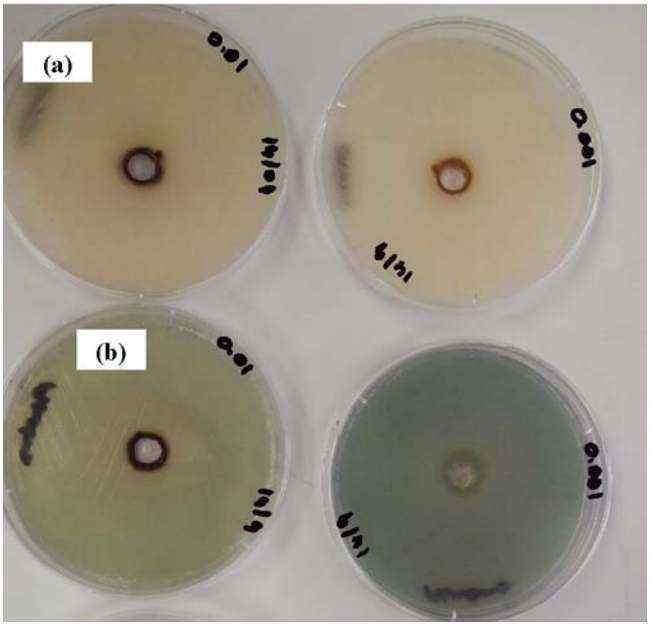

Figure 9. Illustration of the inhibition of bacterium growth by cup plate experiment. In this figure, (a) *P. aeruginosa* and (b) *B. licheniformis* were tested with nanoparticle obtained from 10^{-2} M and 10^{-3} M $AgNO_3$ solutions and the inhibition diameters are as shown in Table 2

Table 3. Assessment of the antimicrobial effect of the AgNPs (a), Amoxicilin (b) and Ciprofloxacin (c) based of turbidity visualization of the culture and bacteria count on solid Agar plate. Values in brackets represent bacteria counts (CFU × 105/mL) after 24 h culture. Positive control presents culture liquid without nanoparticles and negative control is the culture without bacteria

(a)	AgNPs (in M)					Controls	
Microorganisms	4×10^{-4}	4×10^{-5}	4×10^{-6}	4×10^{-7}	4×10^{-8}	Positive	Negative
Pseudomonas aeruginosa	– (0)	– (0)	+ (8)	++ (45)	++ (1200)	+++ (3500)	– (0)
Bacillus licheniformis	– (0)	– (0)	– (4)	– (80)	++ (520)	+++ (2500)	– (0)

(b)	Amoxicilin concentration (M)					Controls	
Microorganisms	5×10^{-6}	5×10^{-7}	5×10^{-8}	5×10^{-9}	5×10^{-10}	Positive	Negative
Pseudomonas aeruginosa	– (0)	– (0)	– (8)	+ (780)	++ (16000)	+++ (24000)	– (0)
Bacillus licheniformis	– (0)	– (0)	– (0)	+ (48)	++ (1180)	+++ (16400)	– (0)

(c)	Ciprofloxacin concentration (in M)					Controls	
Microorganisms	10^{-6}	10^{-7}	10^{-8}	10^{-9}	10^{-10}	Positive	Negative
Pseudomonas aeruginosa	– (0)	– (0)	– (3.6)	+ (1800)	+ (2400)	+++ (24000)	– (0)
Bacillus licheniformis	– (0)	– (0)	– (0)	+ (3.2)	++ (860)	+++ (16400)	– (0)

Table 4. Minimum inhibitory concentration that inhibit bacteria growth, based on visual turbidity or bacteriostatic effect (MIC, in M), and minimum inhibitory concentration that inhibit growth in solid plate culture or bactericidal effect (MBC, in M)

	AgNPs		Amoxicilin		Ciprofloxacin	
Microorganisms	MIC	MBC	MIC	MBC	MIC	MBC
Pseudomonas aeruginosa	4×10^{-5}	4×10^{-5}	5×10^{-7}	5×10^{-8}	10^{-8}	10^{-7}
Bacillus licheniformis	4×10^{-7}	4×10^{-5}	5×10^{-8}	5×10^{-8}	10^{-8}	10^{-9}

CONCLUSIONS

On the basis of the findings of this investigation, the following conclusions are drawn:

– AgNPs can be synthesized at room temperature by mixing aqueous solution of $AgNO_3$ with Strawberry fruit extract.

– The formation of AgNPs and the size of the nanoparticles are influenced by $AgNO_3$ and SBFE concentrations as well as reaction time. 5 mL SBFE with 0.01 M $AgNO_3$ produced stable and bigger AgNPs at 18 days reaction time.

– AgNPs exhibit inhibiting influence on *Pseudomonas aeruginosa* and *Bacillus licheniformis* growth. The antibacterial activity is a function of concentration; however its inhibition profile is lower than that of the reference antibiotic amoxicillin and ciprofloxacin.

LITERATURE CITED

1. Chowdhury, I.H., Ghosh, S., Roy, M. & Naskar, M.K. (2015). Green synthesis of water-dispersible silver nanoparticles at room temperature using green carambola (star fruit) extract. *J. Sol–Gel Sci. Techno*l., 73, 199–207. DOI: 10.1007/s10971-014-3515-1.

2. Ravi, S.S., Christena, L.R., SaiSubramanian, N. & Anthony, S.P. (2013). Green synthesized silver nanoparticles for selective colorimetric sensing of Hg^{2+} in aqueous solution at wide pH range. *Analyst*. 138, 4370–4377. DOI: 10.1039/c3an00320e.

3. Li, L., Zhou, G., Cai, J., Chen, J., Wang, P., Zhang, T., Ji, M. & Gu, N. (2014). Preparation and characterization of a novel nanocomposite: silver nanoparticles decorated cerasome. *J. Sol–Gel Sci. Technol*. 69, 199–206. DOI: 10.1007/s10971-013-3204-5.

4. Gopinath, V., MubaraAli, D., Priyadarshini, S., Priyadharshini, N.M., Thajuddin, N. & Velusamy, P. (2012). Biosynthesis of silver nanoparticles from *Tribulus terrestris* and its antimicrobial activity: a novel biological approach, *Coll. Surf. B: Biointerf*. 96, 69–74. DOI:10.1016/j.colsurfb.2012.03.023.

5. Bindhu, M.R. & Umadevi, M. (2013). Synthesis of monodispersed silver nanoparticles using *Hibiscus cannabinus* leaf extract and its antimicrobial activity. *Spectrochimica Acta Part A: Molecu. Biomole. Spectrosc.* 101, 184–190. DOI:10.1016/j.saa.2012.09.031.

6. Kruis, F., Fissan, H. & Rellinghaus, B. (2000). Sintering and evaporation characteristics of gas-phase synthesis of size--selected PbS nanoparticles. *Mater. Sci. Eng. B*. 69, 329–334. DOI: 10.1016/S0921-5107(99)00298-6.

7. Magnusson, M., Deppert, K., Malm J., Bovin J. & Samuelson, L. (1999), Gold nanoparticles: production, reshaping, and thermal charging, *J. Nanoparticle Res.* 1, 243–251. DOI: 10.1023/A:1010012802415.

8. Goudarzi, M., Zarghami, Z. & Salavati-Niasari, M. (2016). Novel and solvent-free cochineal-assisted synthesis of Ag–Al_2O_3 nanocomposites via solid-state thermal decomposition route: characterization and photocatalytic activity assessment. *J. Mater. Sci. Mater. Electron*. 27, 9789–9797. DOI: 10.1007/s10854-016-5044-x.

9. Oliveira, M., Ugarte, D., Zanchet, D. & Zarbin, A. (2005), Influence of synthetic parameters on the size, structure, and stability of dodecanethiol-stabilized silver nanoparticles. *J. Coll. Interf. Sci*. 292, 429–435. DOI:10.1016/j.jcis.2005.05.068.

10. Khomutov, G. & Gubin, S. (2002). Interfacial synthesis of noble metal nanoparticles. *Mater. Sci. Eng. C.* 22, 141–146. DOI: 10.1016/S0928-4931(02)00162-5.

11. Mousavi-Kamazani, M. Salavati-Niasari, M., Mostafa-Hosseinpour-Mashkani, S. & Goudarzi, M. (2015). Synthesis and characterization of $CuInS_2$ quantum dot in the presence of novel precursors and its application in dyes solar cells. *Mater. Lett*. 145, 99–103. DOI: 10.1016/j.matlet.2015.01.076.

12. Joerger, R., Klaus, T. & Granqvist, C. (2000). Biologically produced silver-carbon composite materials for optically functional thin-film coatings. *Adv. Mater.* 12, 407–409. DOI: 10.1002/(SICI)1521-4095(200003)12:6<407::AID-ADMA-407>3.0.CO;2-O.

13. Shankar, S., Ahmad, A., Paricha, R. & Sastry, M. (2003). Bioreduction of chloroaurate ions by geranium leaves and its endophytic fungus yields gold nanoparticles of different shapes. *J. Mater. Chem.* 13, 1822–1826. DOI: 10.1039/b303808b.

14. Goudarzi, M., Mousavi-Kamazani, M. & Salavati-Niasari, M. (2017). Zinc oxide nanoparticles: solvent-free synthesis, characterization and application as heterogeneous nanocatalyst for photodegradation of dye from aqueous phase. *J. Mater. Sci, Mater. Electron.* 28, 8423–8428. DOI: 10.1007/s10854-017-6560-z.

15. Mousavi-Kamazani, M. Salavati-Niasari, M., Goudarzi, M. & Zarghami, Z. (2017). Hydrothermal synthesis of $CdIn_2S_4$ nanostructures using new starting reagent for elevating solar cells efficiency. *J. Mol. Liq*. 242, 653–661. DOI: 10.1016/j.molliq.2017.07.059.

16. Shahverdi, A.R., Minaeian, S., Shahverdi, H.R., Jamalifar, H. & Nohi, A.A. (2007). Rapid synthesis of silver nanoparticles using culture supernatants of Enterobacteria: a novel biological approach. *Process Biochem*. 42, 919–923. DOI: 10.1016/j.procbio.2007.02.005

17. Varshney, R., Mishra, A.N., Bhadauria, S. & Gaur, M.S. (2009). A novel microbial route to synthesize silver nanoparticles using fungus *Hormoconis resinae*. *Digest. J. Nanomater. Biostruct*. 4, 349–355.

18. Durán, N., Marcato, P.D., Alves, O.L., De Souza, G.I.H. & Esposito, E. (2005). Mechanistic aspects of biosynthesis of silver nanoparticles by several *Fusarium oxysporum* strains. *J. Nanobiotechnol*. 3, 1–7. DOI: 10.1186/1477-3155-3-8.

19. Vigneshwaran, N., Nachane, R.P., Balasubramanya, R.H. & Varadarajan, P.V. (2006). A novel one-pot 'green'synthesis of stable silver nanoparticles using soluble starch, *Carbohyd. Res*. 341, 2012–2018. DOI: 10.1016/j.carres.2006.04.042.

20. Ghaffari-Moghaddam, M. & Hadi-Dabanlou, R. (2014). Plant mediated green synthesis and antibacterial activity of silver nanoparticles using *Crataegus douglasii* fruit extract, *J. Ind. Eng. Chem.* 20, 739–744. DOI: 10.1016/j.jiec.2013.09.005.

21. Padalia, H., Moteriya, P. & Chanda, S. (2014). Green synthesis of silver nanoparticles from marigold flower and its synergistic antimicrobial potential *Arab. J. Chem.* DOI: 10.1016/j.arabjc.2014.11.015.

22. Goudarzi, M., Mir, N., Mousavi-Kamazani, M., Bagheri, S. & Salavati-Niasari, M. (2016).Biosynthesis and characterization of silver nanoparticles prepared from two novel natural precursors by facile thermal decomposition methods. *Sci. Rep.* 6, 32539. DOI: 10.1038/srep32539.

23. Rai, M., Yadav, A., and Gade, A. (2009). Silver nanoparticles as a new generation of antimicrobials. *Biotechnol. Adv*. 27, 76–83. DOI: 10.1016/j.biotechadv.2008.09.002.

24. Lara, H.H., Garza-Trevino, E.N., Ixtepan-Turrent, L. & Singh, D.K. (2011). Silver nanoparticles are broad-spectrum bactericidal and virucidal compounds. *J. Nanobiotechnol*. 9, 1–8. DOI: 10.1186/1477-3155-9-30.

25. Chernousova, S. & Epple, M. (2013), Silver as antibacterial agent: ion, nanoparticle, and metal. *Angew Chem. Int. Ed. Eng*. 52, 1636–1653, https://doi.org/10.1002/anie.201205923.

26. Ahmed, M.J., Murtaza, G., Mehmood, A. & Bhatti, T.M. (2015). Green synthesis of silver nanoparticles using leaves extract of *Skimmia laureola*: Characterization and antibacterial activity. *Mater. Lett*. 153, 10–13. DOI: 10.1016/j.matlet.2015.03.143.

27. Manganaris, G.A., Goulas, V., Vicente, A.R. & Terry, L.A. (2014). Berry antioxidants: small fruits providing large benefits. *J. Sci. Food Agric.* 94, 825–33. DOI: 10.1002/jsfa.6432.

28. Basu, A., Nguyen, A., Betts, N.M. & Lyons, T.J. (2014). Strawberry as a functional food: an evidence-based review. *Critical Rev. Food Sci. Nutri.* 54, 790–806. DOI: 10.1080/10408398.2011.608174.

29. Giampieri, F., Alvarez-Suarez, J. M., Mazzoni, L., Romandini, S., Bompadre, S., Diamanti, J., Capocasa, F., Mezzetti, B., Quiles, J.L., Ferreiro, M.S., Tulipani, S. & Battino, M. (2013). The potential impact of strawberry on human health. *Nat. Prod. Res.* 27, 448–55. DOI: 10.1080/14786419.2012.706294.

30. Rios, J.L., Recio, M.C. & Villar, A. (1988). Screening methods for natural products with antimicrobial activity: a review of the literature. *J. Ethnopharmacol*. 23, 127–149. DOI: 10.1016/0378-8741(88)90001-3.

31. Wei, D., Sun, W., Qian, W., Ye, Y. & Ma, X. (2009). The synthesis of chitosan-based silver nanoparticles and their antibacterial activity. *Carbohyd. Res*. 344, 2375–2382. DOI: 10.1016/j.carres.2009.09.001.

32. Solomon, M.M. & Umoren, S.A. (2016), In-situ preparation, characterization and anticorrosion property of polypropylene glycol/silver nanoparticles composite for mild steel corrosion in acid solution. *J. Coll. Interf. Sci.* 462, 29–41. DOI: 10.1016/j.jcis.2015.09.057.

33. Stamplecoskie, K.G. & Scaiano, J.C. (2010). Light emitting diode irradiation can control the morphology and optical properties of silver nanoparticles. *J. Am. Chem. Soc.* 132, 1825–1827. DOI: 10.1021/ja910010b.

34. Solomon, M.M., Umoren, S.A. & Abai, E.J. (2015). Poly(methacrylic acid)/silver nanoparticles composites: In-situ preparation, characterization and anticorrosion property for mild steel in H_2SO_4 solution. *J. Mol. Liq.* 212, 340–351. DOI: 10.1016/j.molliq.2015.09.028.

35. Prathna, T.C., Chandrasekaran, N., Raichur, A.M. & Mukherjee, A. (2011). Biomimetic synthesis of silver nanoparticles by *Citrus limon* (lemon) aqueous extract and theoretical prediction of particle size. *Coll. Surf. B: Biointerf*. 82, 152–159. DOI: 10.1016/j.colsurfb.2010.08.036.

36. Jagadeesh, B.H., Prabha, T.N. & Srinivasan, K. (2004). Activities of β-hexosaminidase and α-mannosidase during development and ripening of bell capsicum (*Capsicum annuum* var.variata*). Plant Sci*. 167, 1263–1271. DOI: 10.1016/j.plantsci.2004.06.031.

37. Cordenunsi, B.R., Oliveira do Nascimento, J.R., Genovese, M.I. & Lajolo, F.M. (2002). Influence of cultivar on quality parameters and chemical composition of strawberry fruits grown in Brazil, *J. Agric. Food Chem.* 50, 2581–2586. DOI: 10.1021/jf011421i

38. Zayed, M.F., Eisa, W.H., Abdel-Moneam, Y.K., El-Kousy, S.M. & Atia, A. (2015). Ziziphus spina-christi based bio-synthesis of Ag nanoparticles. *J. Ind. Eng. Chem*. 23, 50–56. DOI: 10.1016/j.jiec.2014.07.041

39. Lateef, A., Azeez, M.A., Asafab, T.B., Yekeen, T.A., Akinboro, A., Oladipo, I.C., Azeez, L., Ajibade, S.E., Ojo, S.A., Gueguim-Kana, E.B. & Beukes, L.S. (2016). Biogenic synthesis of silver nanoparticles using a pod extract of *Cola nitida*: Antibacterial and antioxidant activities and application as a paint additive. *J. Taibah Univer Sci.* 10, 551–562. DOI: 10.1016/j.jtusci.2015.10.010.

40. Solomon, M.M., Umoren, S.A. & Ebenso, E.E. (2015). Polypropylene glycol-silver nanoparticle composites: a novel anticorrosion material for aluminum in acid medium, *J. Mater. Eng. Perform.* 24, 4206–4218. DOI: 10.1007/s11665-015-1716-6.

41. Rao, Y.S., Kotakadi, V.S., Prasad, T.N.V.K.V., Reddy, A.V. & Sai Gopal, D.V.R. (2013). Green synthesis and spectral characterization of silver nanoparticles from Lakshmi tulasi (*Ocimum sanctum*) leaf extract. *Spectrochim. Acta Part A: Mol. Biomol. Spec.* 103, 156–159. DOI: 10.1016/j.saa.2012.11.028.

42. Edison T.J.I. & Sethuraman M.G. (2012). Instant green synthesis of silver nanoparticles using *Terminalia chebula* fruit extract and evaluation of their catalytic activity on reduction of methylene blue. *Process Biochem.* 47, 1351–1357. DOI: 10.1016/j.procbio.2012.04.025.